ELSEVIER

Deep-Sea Research II 51 (2004) 1333–1350

DEEP-SEA RESEARCH
PART II

www.elsevier.com/locate/dsr2

Factors influencing the distribution, biomass, and productivity of phytoplankton in the Scotia Sea and adjoining waters

O. Holm-Hansen[a,*], M. Naganobu[b], S. Kawaguchi[b,1], T. Kameda[b], I. Krasovski[c], P. Tchernyshkov[c], J. Priddle[d,2], R. Korb[d], M. Brandon[d], D. Demer[e], R.P. Hewitt[e], M. Kahru[a], C.D. Hewes[a]

[a]*Scripps Institution of Oceanography, University of California at San Diego, La Jolla, CA 92093, USA*
[b]*National Research Institute of Far Seas Fisheries, 5-7-1 Orido, Shimizu, Shizuoka-pref. 424-8633, Japan*
[c]*Atlantic Scientific Research Institute for Marine Fisheries and Oceanography (AtlantNIRO). 5, Dmitry Donskoy st., Kaliningrad, 236000, Russia*
[d]*British Antarctic Survey, NERC, High Cross, Madingley Road, Cambridge CB3 OET, UK*
[e]*Southwest Fisheries Science Center, National Oceanic & Atmospheric Administration, P.O. Box 271, La Jolla, CA 92038, USA*

Accepted 18 June 2004
Available online 16 September 2004

Abstract

During January and February 2000 four research vessels, from Russia, the UK, Japan, and the United States, conducted an oceanographic survey with 137 hydrographic stations within the Scotia Sea and adjoining waters as part of a survey sponsored by the Commission for the Conservation of Antarctic Marine Living Resources (CCAMLR) to estimate the biomass and distribution of Antarctic krill in the Scotia Sea. Chlorophyll-*a* (Chl-*a*) measurements showed great variability in phytoplankton biomass within the Scotia Sea, with some areas having among the lowest Chl-*a* concentrations found in Antarctic waters ($<0.1\,mg\,m^{-3}$ in surface waters) while other areas were among the richest with $>10\,mg\,m^{-3}$. This paper describes the distribution and concentration of Chl-*a* in the upper 100 m of the water column and relates the Chl-*a* profiles at individual stations to profiles of upper water-column stability, to the depth of the upper mixed layer, and to the mixing of different water masses. The 58 stations with the lowest Chl-*a* values in surface waters also had low values for integrated Chl-*a* ($33.9\pm19.5\,mg\,m^{-2}$) and a Chl-*a* maximum at depths of between 70 and 90 m, in contrast to all other stations where deep Chl-*a* maxima did not occur. The *T*/*S* diagrams at many of these stations were indicative of Antarctic Circumpolar Current (ACC) waters. The central Scotia Sea and areas to the west and north of South Georgia had significantly higher integrated Chl-*a* values ($98.1\pm46.0\,mg\,m^{-2}$, $n=57$), in addition to five stations with very high Chl-*a* values (mean of $359\pm270\,mg\,m^{-2}$). The mean rate of integrated primary production, which was estimated using the Chl-*a* data and the mean incident solar radiation measured from previous cruises as well as from satellite data, was estimated to be 994 mg carbon m^{-2} day^{-1}. The temperature profiles at these stations suggested that considerable interleaving and mixing of water

*Corresponding author.
E-mail address: oholmhansen@ucsd.edu (O. Holm-Hansen).
[1]Present address: Australian Antarctic Division, Channel Highway, Kingston, Tasmania 7050, Australia.
[2]Present address: Science Training and Education Partnership, Scolt House, 59 High Street, Barrington CB2 5QX, UK.

0967-0645/$ - see front matter Published by Elsevier Ltd.
doi:10.1016/j.dsr2.2004.06.015

types had occurred, which was also evident in the T/S diagrams, which indicated mixing of ACC waters with coastal waters originating from Bransfield Strait or the Weddell Sea. There was no significant correlation between integrated Chl-*a* values and the profiles of upper water column stability or the depth of the upper mixed layer. The spatial variability in phytoplankton biomass within the Scotia Sea is discussed in relation to the hypothesis that low iron concentrations are the major factor controlling phytoplankton biomass in these pelagic Antarctic waters and that concentrations of iron available for phytoplankton uptake are strongly influenced by fronts and the mixing of different water masses.
Published by Elsevier Ltd.

1. Introduction

The Scotia Sea has been one of the most productive areas in the Southern Ocean for the harvest of krill, crabs, fish, seals, and whales. At present, the commercial harvesting of krill in the Southern Ocean is confined almost entirely to the Scotia Sea and its adjacent waters. This must be supported by rich food reservoirs and suggests that phytoplankton biomass and associated rates of primary production in the Scotia Sea must be high relative to most other pelagic regions of the Southern Ocean. In this paper, rates of integrated primary production are estimated such that the phytoplankton data can be expressed in units of organic carbon, which is the biomass unit commonly used in models of food chain dynamics. Except for those relatively small shelf regions of the Scotia Arc, the Scotia Sea is deep (2000–4000 m), with some isolated sea mounts or plateaus rising to depths of <2000 m. Although many review articles on Antarctic productivity characterize the pelagic regions of the Southern Ocean as having relatively low phytoplankton biomass compared to regions over the continental shelf, El-Sayed and Weber (1982) commented on the spatial and temporal variability of phytoplankton biomass in the Scotia Sea and pointed out that phytoplankton blooms may occasionally occur in deep oceanic waters (see also Sullivan et al., 1993). Such field data are supported by satellite imagery of chlorophyll-*a* (Chl-*a*), which shows that mean Chl-*a* concentrations are considerably higher in the Scotia Sea than in most pelagic waters surrounding Antarctica (see Fig. 1). It is evident from Fig. 1 that the Scotia Sea includes areas of very low Chl-*a* concentration, with concentrations of $\sim 0.1\,\mathrm{mg\,m^{-3}}$ or less in surface waters, and other areas of very high concentration of $\sim 10\,\mathrm{mg\,m^{-3}}$ or more.

The spatial variability shown in Fig. 1 probably results from differences in the physical and chemical properties of the upper water column that influence the distribution and growth of phytoplankton. Despite its importance and the interest in the Scotia Sea, there had not been any extensive synoptic ship surveys of this region prior to the CCAMLR 2000 Survey. Several research projects have included a few transects through the Scotia Sea (e.g., El-Sayed and Weber, 1982; Fisheries Agency, 1989; Foster and Middleton, 1984; Hayes et al., 1984) or have undertaken detailed studies in a relatively small area (e.g., de Baar et al., 1990), but such projects do not provide the data base of physical and biological measurements for the area as a whole that are needed to understand why the Scotia Sea is such a productive area. The temporal and spatial distribution of Chl-*a* in the surface waters of the Scotia Sea during the CCAMLR 2000 Survey is described by Holm-Hansen et al. (2004). However, satellite imagery of surface Chl-*a* concentration does not permit an examination of the processes and factors responsible for such biological variability. The four vessels that took part in the CCAMLR 2000 Survey obtained data on the distribution and concentration of Chl-*a* in the upper 100 m of the water column at 137 hydrographic stations, in addition to CTD measurements at each of these stations. The primary objective of this paper is to use these data, together with existing knowledge of the different water masses within the Scotia Sea, to establish the factors and processes most likely to be responsible for the spatial variability in phytoplankton biomass within the Scotia Sea.

2. Materials and methods

The priorities set by the CCAMLR program, as well as time and equipment constraints, did not permit shipboard measurement of primary

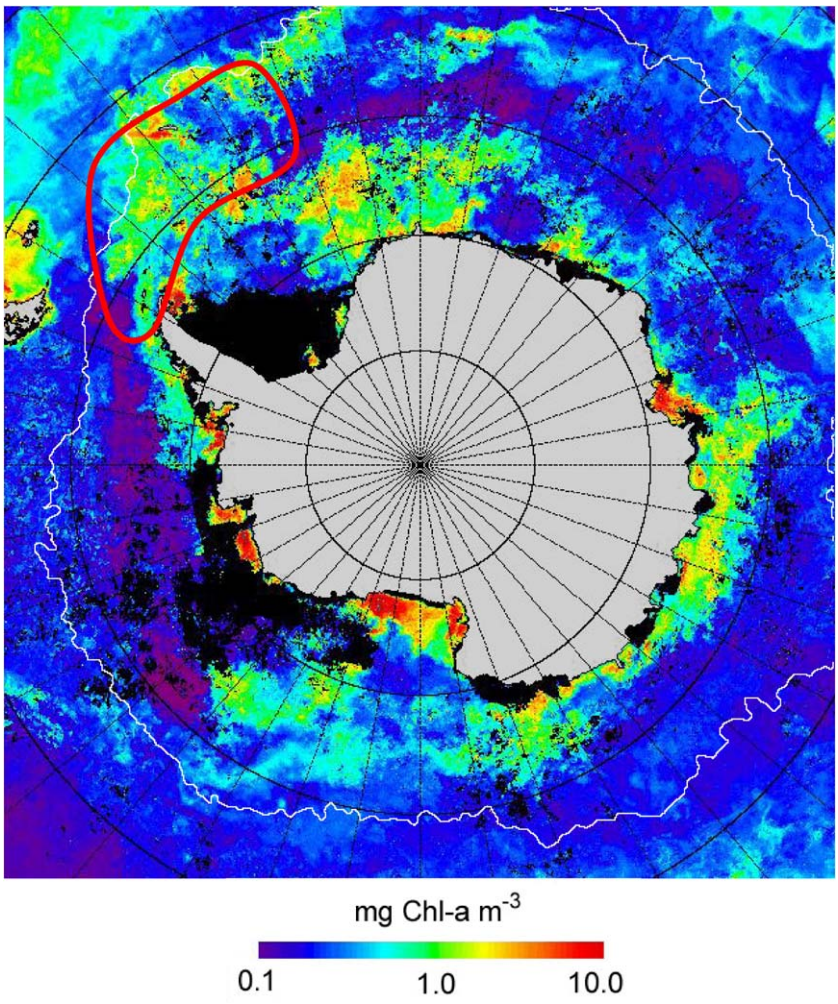

Fig. 1. Mean surface Chl-*a* concentration in the Southern Ocean during January and February 2000. Data are derived from the Sea-viewing Wide Field-of-view Sensor (SeaWiFS; McClain et al., 1998) using the standard OC4v2 chlorophyll algorithm (O'Reilly et al., 1998, 2000). The area outlined in red shows the approximate region surveyed during the CCAMLR 2000 Survey. The jagged white line shows the location of the 4 °C isotherm, which indicates the approximate position of the Polar Front. Areas shown in black have insufficient data due to ice cover or to open water areas with extensive cloud cover.

production rates, light attenuation in the water column, or measurement of iron (Fe) concentrations in seawater samples.

2.1. Ship tracks and station locations

Fig. 2A shows the locations of the 137 hydrographic stations at which Chl-*a* measurements were made. Although most of the stations were located within the Scotia Sea, some were located to the north of South Georgia, to the east of the South Sandwich Islands, in the northern Weddell Sea, in Bransfield Strait, and in Drake Passage waters. All sampling occurred between January 11 and February 11, 2000. The ships involved were the R./V. *Atlantida* (Russia) from January 17 to February 1, the R.V. *Kaiyo Maru* (Japan) from January 11 to February 6, the R.R.S. *James Clark Ross* (UK) from January 16 to February 11, and the US-chartered R.V. *Yuzhmorgeologiya*

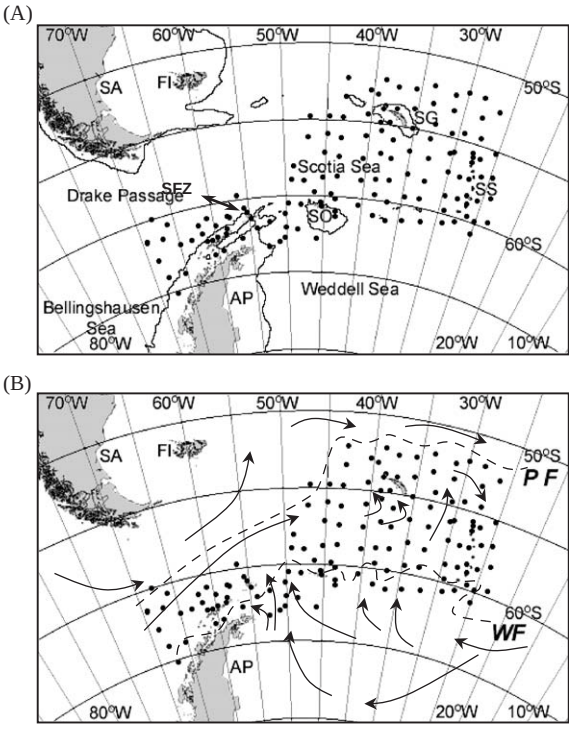

Fig. 2. (A) The Scotia Sea and adjoining waters. The filled circles show the location of the 137 hydrographic stations where Chl-*a* measurements were made. The thin black line shows the 1000 m isobath. SA: South America; FI: Falkland Islands; AP: Antarctic Peninsula; SO: South Orkney Islands; SG: South Georgia; SS: South Sandwich Islands; SFZ: Shackleton Fracture Zone (double-headed arrow). (B) The Scotia Sea and adjoining waters with the approximate location of the Polar Front (PF) and the Weddell Front (WF) during the CCAMLR 2000 Survey, and the general flow of surface waters indicated by arrows.

(Russia) from January 16 to February 4. Transects were generally north–south, starting in the east and moving to the west. Station coordinates and dates are as described by Watkins et al. (2004).

2.2. Water samples

Water samples were obtained at standard depths using Niskin bottles attached to the CTD-profiling units, although the number of depths sampled at each station varied from ship to ship. Surface samples were obtained by bucket. Chl-*a* concentrations were measured at 41 stations by scientists aboard the *James Clark Ross*; at 25 of these stations, sampling depths generally included 0, 6, 20, 30, 40, 60, 80, 100, and 125 m, and at the remaining 16 stations, samples were obtained at 0 and 30 m only because sampling was concentrated at sub-euphotic zone depths at deep hydrographic stations. Chl-*a* concentrations were measured at 27 stations from the *Atlantida*, with sampling depths at 0, 10, 20, 30, 50, 75, and 100 m. Chl-*a* concentrations were measured at 38 stations from the *Kaiyo Maru*, with sampling depths at 0, 10, 20, 30, 50, 75, 100, 150, and 200 m. Chl-*a* concentrations were measured at 31 stations from the *Yuzhmorgeologiya*, with sampling depths at 5, 30, 100, and 150 m. No prefilter was used when taking water from the Niskin bottles for measurement of Chl-*a* concentration.

2.3. Measurement of chlorophyll-a

Water samples, which varied from 100 to 500 ml depending on the expected Chl-*a* concentration, were filtered either through Whatman GF/F glass fiber filters (USA, UK, Japan) or through cellulose acetate filters of Synpor ♯6 type with 0.45 μm pores or Sartorius filters with 0.45 μm pores (Russia). A differential vacuum of 25 cm Hg or less was used in all filtrations. Photosynthetic pigments were extracted by immersion of the filters in 10 ml of 90% acetone. After some hours in the dark (usually 24 h), the samples were shaken and centrifuged. The concentrations of Chl-*a* and phaeophytin in the supernatants were determined by measuring fluorescence before and after acidification (Holm-Hansen et al., 1965). All fluorometers were calibrated against purified Chl-*a* standards. Integrated Chl-*a* values (0 to 100 m) were determined by the trapezoidal summing method for the 90 stations at which Chl-*a* concentrations were measured at six to eight depths between 0 and 100 m. The integrated Chl-*a* values for the other 47 stations (16 *James Clark Ross*; 31 *Yuzhmorgeologiya*) were estimated by applying an equation relating surface Chl-*a* concentration to the integrated Chl-*a* value.

2.4. Physical data

Vertical profiles of temperature and salinity in the upper water column were obtained from profiling CTD units; see Brandon et al. (2004) for a description of instrumentation used. Two methods were used to estimate the lower depth of the upper mixed layer (UML); an objective computational method that determined when sigma-*t* increased by >0.05 over a 5-m depth interval (Mitchell and Holm-Hansen, 1991) and a subjective method based on visual examination of temperature, salinity, and water density profiles. A UML could not be determined for all stations because some showed no significant change in density in the upper 100 m, while others showed a slow but regular increase in density with depth.

2.5. Estimation of primary production rates

As there were no direct measurements of photosynthetic rates during the CCAMLR 2000 Survey, two indirect methods were applied to the Chl-*a* values to estimate rates of primary production.

The first method used the 'Photosynthetic Efficiency' value (0.32) obtained during the RACER program from in situ incubation of samples, and measurement of the integrated Chl-*a* concentration in the euphotic zone and the daily photosynthetic available radiation (PAR) incident upon the ocean surface (Holm-Hansen and Mitchell, 1991). The equation used to estimate integrated primary production at the CCAMLR 2000 Survey stations was the following:

$$\text{mg carbon fixed m}^{-2}\,\text{day}^{-1} = 0.32(\text{mg Chl-}a\,\text{m}^{-2}) \times (\text{Einsteins m}^{-2}\,\text{day}^{-1}).$$

Mean incident PAR during the period of the CCAMLR 2000 Survey was estimated at 43 Einsteins $\text{m}^{-2}\,\text{day}^{-1}$. This value was the average of incident PAR estimated from satellite data (41 Einsteins $\text{m}^{-2}\,\text{day}^{-1}$, M. Kahru, co-author, unpublished data) and the multi-year average (44 Einsteins $\text{m}^{-2}\,\text{day}^{-1}$) obtained by direct measurement during previous studies around Elephant Island during January and February (O. Holm-Hansen and C.D. Hewes, co-author, unpublished data). It should be noted that the Photosynthetic Efficiency value is based on the integrated Chl-*a* value for the entire euphotic zone, whereas the calculations for primary production using the CCAMLR 2000 Survey data are based on the integrated Chl-*a* values between 0 and 100 m depth. As attenuation of solar radiation in the water column was not measured during the CCAMLR 2000 Survey, it was not possible to estimate the rate of primary production based on the depth of the 1% light level at each station. Light attenuation in the water column has, however, been routinely measured during the Antarctic Marine Living Resources (AMLR) program and the mean depth for the 1% light level around Elephant Island and Drake Passage was 90 m (Helbling et al., 1995). As there is relatively little Chl-*a* between 90 and 100 m, using the integrated Chl-*a* value to 100 m rather than to the depth of the euphotic zone will result in a slight overestimation of integrated primary production for the CCAMLR 2000 stations.

The second method used the Vertically Generalized Production Model (VGPM) of Behrenfeld and Falkowski (1997), which was developed for use with satellite-based estimates of Chl-*a* concentration, temperature, and PAR. The present calculations of primary productivity, however, are based on the CCAMLR 2000 data set for surface Chl-*a* concentration and water temperature (instead of satellite-derived values) and the mean PAR value of 43 Einsteins $\text{m}^{-2}\,\text{day}^{-1}$. CTD data were not available for nine of the CCAMLR 2000 stations, so the total number of values estimated by the VGPM method was 128.

3. Results

3.1. Phytoplankton distribution and concentration

Chl-*a* concentrations in surface waters throughout the study area ranged from 0.06 to 14.6 mg m^{-3}, with a mean of 1.16 ± 1.57 mg m^{-3}. Fig. 3 shows the distribution of surface Chl-*a* concentration according to three categories: <0.5, 0.5–1.0, and >1.0 mg m^{-3}. The 54 stations with

the lowest concentrations ($<0.5\,mg\,m^{-3}$) were mainly in Drake Passage, the Weddell Sea outflow between the South Orkney Islands and the Antarctic Peninsula, around the South Sandwich Islands, and to the east of South Georgia. The 52 stations with the highest concentrations ($>1.0\,mg\,m^{-3}$) were at the eastern end of Bransfield Strait, in the central Scotia Sea, and to the south, west, and north of South Georgia. Of these, the 24 with the highest values ($>2.0\,mg\,m^{-3}$) were clustered in the central Scotia Sea (55–60° S, 40–45° W) and near South Georgia, with three additional stations near the South Shetland Islands. Most of the 31 stations with Chl-*a* values of 0.5–1.0 $mg\,m^{-3}$ occurred between the South Sandwich Islands and South Georgia, and near the South Orkney Islands.

There is a good correlation between surface Chl-*a* values and integrated Chl-*a* (0–100 m; see Fig. 4). The integrated Chl-*a* values ranged from 9 (in Drake Passage) to 836 $mg\,m^{-2}$ at a relatively shallow station to the southwest of South Georgia. The relationship shown in Fig. 4 was used to estimate integrated Chl-*a* values for the 47 stations that had measured Chl-*a* concentrations for surface waters but an insufficient number of samples with depth to justify integration to 100 m. The mean integrated value for all 137 CCAMLR 2000 stations was $80.6 \pm 86.0\,mg\,Chl\text{-}a\,m^{-2}$.

The Chl-*a* profiles for 121 CCAMLR 2000 stations (16 stations had only one or two Chl-*a* samples) were individually examined and grouped into four categories based on relative changes in Chl-*a* concentration with depth between 0 and 100 m (Fig. 5). Twenty-seven stations (see Fig. 5A) had very low Chl-*a* concentrations in surface waters (mean $0.29 \pm 0.21\,mg\,m^{-3}$) and a deep Chl-*a* maximum at approximately 75 m (mean $0.56 \pm 0.48\,mg\,m^{-3}$). The locations of these stations are shown in Fig. 6A. The 31 stations included in Fig. 5B (locations in Fig. 6B) had slightly higher Chl-*a* concentrations in surface waters (mean $0.36 \pm 0.21\,mg\,m^{-3}$) but no deep Chl-*a* maximum at 75 m (mean $0.31 \pm 0.18\,mg\,m^{-3}$). The most common profiles (58 stations) had fairly high and uniform Chl-*a* concentrations in the UML (mean $1.45 \pm 0.82\,mg\,m^{-3}$ in surface waters), with decreasing concentrations below the UML are shown in Fig. 5C, with the corresponding locations shown in Fig. 6C. The Chl-*a* profiles for the five stations with surface Chl-*a* concentrations $>4.0\,mg\,m^{-3}$ are shown in Fig. 5D (locations in Fig. 6D). The mean integrated Chl-*a* values for

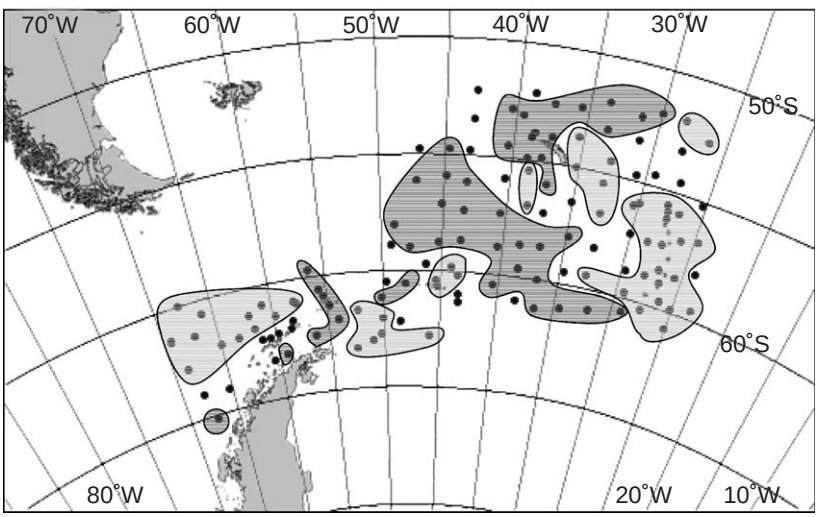

Fig. 3. Chl-*a* concentration in surface waters according to three categories: $<0.5\,mg\,m^{-3}$ (lightly shaded); 0.5 to $1.0\,mg\,m^{-3}$ (no shading); $>1.0\,mg\,m^{-3}$ (dark shading).

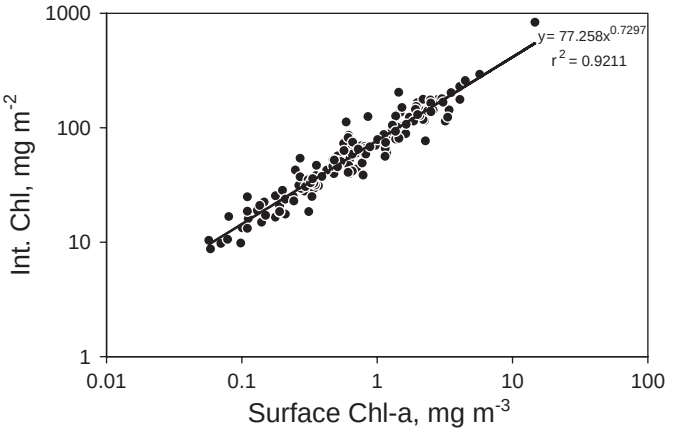

Fig. 4. Relationship between surface Chl-*a* concentration and the integrated values for 0–100 m.

profile types A–D (Fig. 5) were 34.8 ± 23.7, 33.0 ± 16.7, 98.1 ± 46.0, and $359 \pm 270\,\mathrm{mg\,m^{-2}}$, respectively.

3.2. Rates of primary production

The depth-integrated rates of primary production estimated by the two methods described in Section 2.5 are shown in Fig. 7. There is a good correlation between these two independent measurements, but the values based on the equation developed during the RACER program are approximately 1.8 times higher than the values estimated using the VGPM equation. The mean estimated productivity values for the two methods are $994 \pm 1132\,\mathrm{mg\,C\,m^{-2}\,day^{-1}}$ ($n = 137$) and $597 \pm 493\,\mathrm{mg\,C\,m^{-2}\,day^{-1}}$ ($n = 128$), respectively. The major factor responsible for the difference in estimates between these two methods seems to be the integrated Chl-*a* value used for the upper water column. The VGPM method estimates this value ($36\,\mathrm{mg\,Chl\text{-}a\,m^{-2}}$) for the depth of the euphotic zone from surface Chl-*a* concentrations as described by Morel and Berthon (1989), whereas the other method uses values based on shipboard measurements of Chl-*a* concentration (mean $81\,\mathrm{mg\,Chl\text{-}a\,m^{-2}}$). As satellite images of surface Chl-*a* concentration show good agreement with shipboard Chl-*a* measurements (Holm-Hansen et al., 2004) and there is good correlation between surface Chl-*a* and integrated Chl-*a* in the upper 100 m (Fig. 4), spatial variability in the rates of primary production in the Scotia Sea will be fairly similar to the variability in Chl-*a* concentration in surface waters (Fig. 3).

3.3. Chl-a and the depth of the upper mixed layer

As many models of phytoplankton distribution in the water column are based on the depth of the UML and the rate of attenuation of solar radiation (Mitchell et al., 1991; Sakshaug et al., 1991), the profiles of Chl-*a* and water density were examined to evaluate the general assumption that high Chl-*a* concentrations occur mostly in shallow UMLs, and that deep UMLs result in low Chl-a concentrations. The water density profiles for the 128 stations for which CTD data were available were examined and grouped into four categories: shallow UMLs of <30 m, deep UMLs of >50 m, stations with no definable UML as there was a steady increase in density with depth, and stations with little or no increase in density in the upper 100 m. Representative examples of these four categories, together with their corresponding profiles of Chl-*a* concentration, are shown in Fig. 8. For each of the four categories, two stations were selected for which the water density profiles are similar, but which have very different values for integrated Chl-*a*. The two stations with UMLs of approximately 25 m (Fig. 8A) have integrated Chl-*a* values of 19 (close to the South

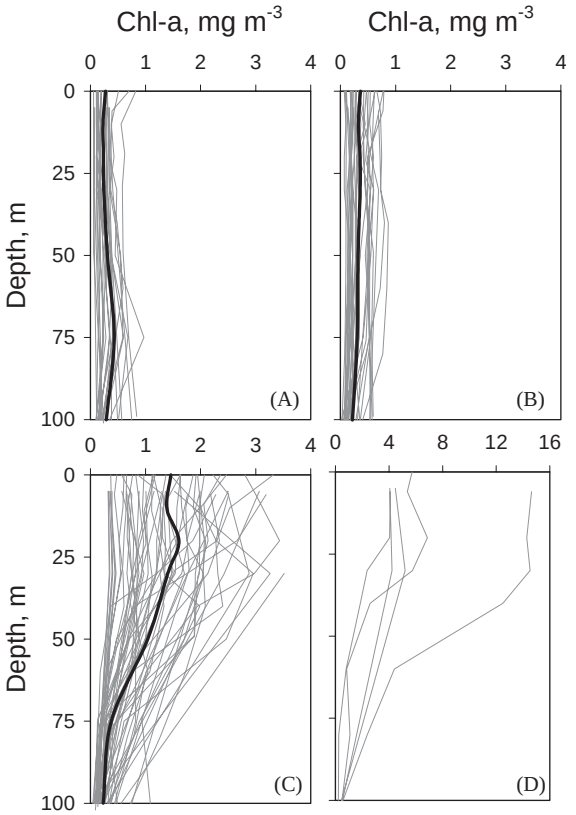

Fig. 5. Chl-*a* profiles within the upper 100 m of the water column. The light lines show the profiles for individual stations, and the dark lines in (A–C) show the mean distribution for all stations in that group. (A) Stations with low Chl-*a* concentrations in surface waters, and a deep Chl-*a* maximum close to 75 m. (B) Stations with low and fairly uniform Chl-*a* concentrations between 0 and 100 m. (C) Stations with highest Chl-*a* concentrations in the upper mixed layer, and rapidly decreasing concentrations below 50 m. (D) Stations with Chl-*a* concentrations $>4.0\,mg\,m^{-3}$ in the upper water column (note change in values for abscissa).

Sandwich Islands) and $142\,mg\,m^{-2}$ (northeast of the South Orkney Islands). The two stations with UMLs of approximately 75 m (Fig. 8B) have integrated Chl-*a* values of 10 (Drake Passage waters) and $140\,mg\,m^{-2}$ (southwest of the South Georgia). The two stations that show a continuous increase in density with depth (Fig. 8C) have integrated Chl-*a* values of 13 (close to the South Sandwich Islands) and $114\,mg\,m^{-2}$ (close to the shelf break north of Elephant island). The two stations that show little or no increase in density with depth (Fig. 8D) have integrated Chl-*a* values of 49 (Bransfield Strait) and $124\,mg\,m^{-2}$ (northwest of the South Orkney Islands).

The lack of a significant relationship between the depth of the UML and the integrated Chl-*a* value is evident when data for all 128 stations are plotted (Fig. 9). The locations of the seven stations with UMLs >100 m were close to the South Orkney Islands, just to the south of Elephant Island, to the north of the South Shetland Islands, and one in the southeast section of Bransfield Strait. Of the eight stations having UMLs between 70 and 87 m, two were located in Drake Passage waters with integrated Chl-*a* values of 10 and $29\,mg\,m^{-2}$, one was to the southeast of Elephant Island, four were to the north and east of South Georgia at the periphery of the sampling grid, and one was in the Scotia Sea at approximately 56° S, 47° W. The richest station ($836\,mg\,Chl\text{-}a\,m^{-2}$) was close to the shelf break to the southwest of South Georgia and had a UML of 22 m. The mean UML depth for all 128 stations was 32 m.

3.4. Temperature profiles

The temperature–depth profiles for the 128 stations for which CTD data were available are shown in Fig. 10. The cluster of profiles with surface temperatures of $<1.0\,°C$ and a temperature minimum of $<-1.0\,°C$ at depths between 80 and 100 m were all located close to the Weddell Front (see Fig. 2B). This cold layer between 50 and 100 m represents the winter remnant of the Antarctic Surface Water, which generally extends from close to the continental shelf northward to the Polar Front and becomes progressively deeper at lower latitudes (Gordon and Baker, 1982; Sievers and Nowlin, 1988). The station with a similar low temperature minimum but with a surface temperature of 2.7 °C (Fig. 10) is typical of pelagic Drake Passage waters to the north of the South Shetland Islands and Elephant Island (Amos, 2001; Holm-Hansen et al., 1994). The two stations marked by dark lines with surface temperatures close to 5.0 °C (Fig. 10) are located in the Polar Frontal Zone and are the only stations that did not show some evidence of a temperature minimum between 30 and 100 m. The temperature

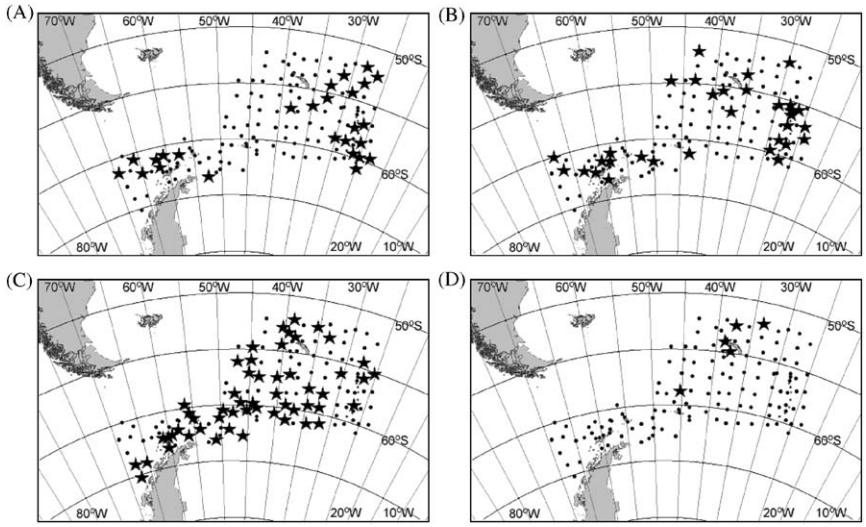

Fig. 6. The location of stations represented by the four groups of Chl-*a* profiles in the upper water column shown in Fig. 5. Circles indicate the hydrographic stations sampled during the CCAMLR 2000 Survey; stars indicate the location of the stations included in Fig. 5(A–D, respectively).

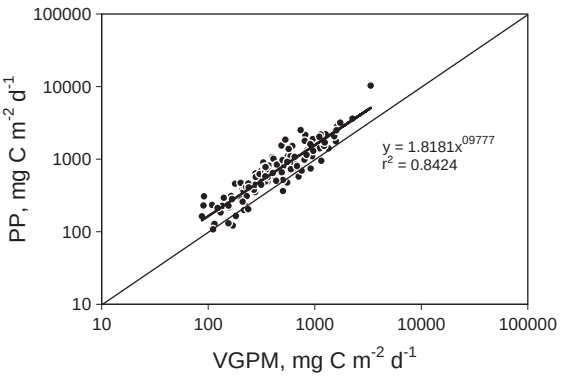

Fig. 7. Relationship between primary production rates estimated using the Vertically Generalized Production Model (VGPM) model of Behrenfeld and Falkowski (1997; *x*-axis) and rates estimated using the Photosynthetic Efficiency value derived from in situ incubations during the RACER program in Antarctic waters (Holm–Hansen and Mitchell, 1991; *y*-axis).

profiles for most of the stations in the Scotia Sea indicate considerable erosion of the temperature minimum layer, suggesting that considerable mixing of different water types had occurred in the upper water column. An example is shown in Fig. 10 by the dashed line with a surface temperature of approximately 2.3 °C (station USA017). Stations indicating complex mixing generally occurred in the southern section of the sampling grid where Weddell Sea waters flow northward into the Scotia Sea. Such stations often had fairly high concentrations of Chl-*a*.

3.5. Physical mixing processes as indicated by temperature/salinity diagrams

The *T*/*S* diagrams for stations in Drake Passage (Fig. 11A) were typical of Drake Passage waters as described by Amos (2001) and Brandon et al. (2004), and show the presence of Antarctic Surface Water, a layer of Winter Water with a temperature minimum (<0.0 °C) at a depth of between 60 and 80 m, and Circumpolar Deep Water at greater depths. The mean surface Chl-*a* concentration at the stations shown in Fig. 11A was 0.15 mg m^{-3}. The *T*/*S* diagrams for all other stations in the Scotia Sea indicate considerable mixing of water masses, as they differ markedly from those for Drake Passage waters. This is illustrated in Fig. 11B, which shows the *T*/*S* diagrams for the 14 stations in the Scotia Sea that had >2.5 mg Chl-*a* m^{-3} in surface waters. The mean Chl-*a* concentration in surface waters at these stations was 4.31 mg m^{-3}.

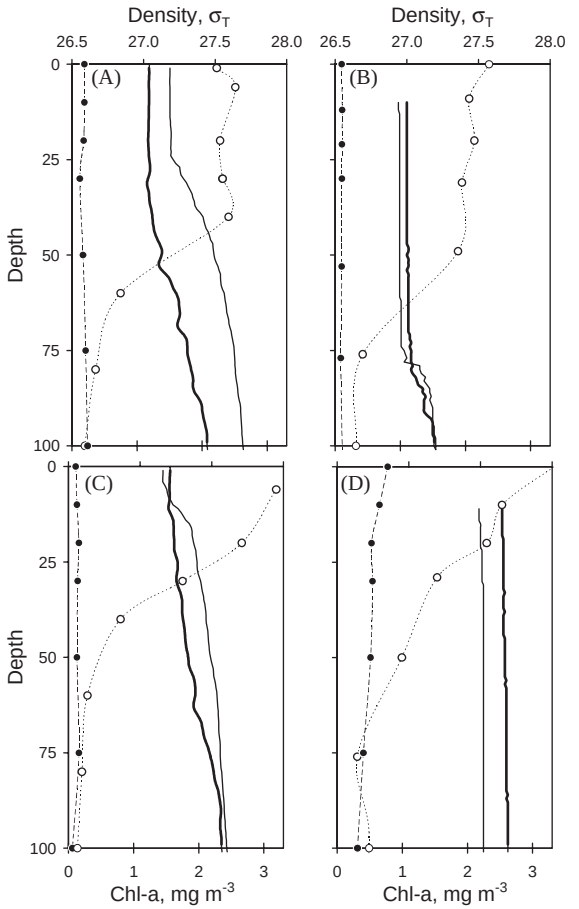

Fig. 8. Representative profiles of water density (sigma-*t*) and Chl-*a* concentration in the upper water column (0–100 m), illustrating the lack of correlation between UML depth and Chl-*a* concentration. Each plot shows the sigma-t profiles for two stations (dark and light continuous lines) and the corresponding Chl-*a* profiles (dashed lines; with the Chl-*a* profiles containing the filled circles corresponding to the sigma-*t* profiles shown by the dark lines). Where the lines do not extend to 0 m, sampling did not extend higher than the indicated depth. (A) Stations with a well formed UML of <30 m; stations shown are AT024 (dark line) and JCR095. (B) Stations with a deep UML (>50 m); stations shown are KM163 (dark line) and KM138. (C) Stations without a distinct UML, with water density increasing slowly with depth; stations shown are AT005 (dark line) and JCR268. (D) Stations with little or no increase in water density between 0 and 100 m; stations shown are KM160 (dark line) and KM145.

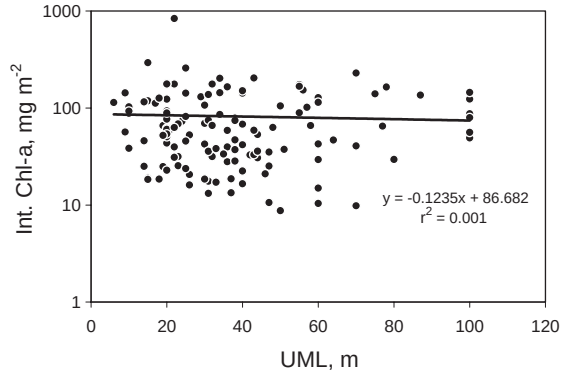

Fig. 9. Lack of correlation between UML depth and the integrated Chl-*a* value (0–100 m) for the 128 stations for which CTD data were available.

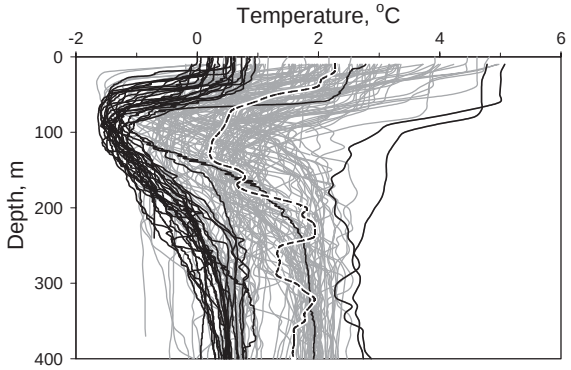

Fig. 10. Temperature profiles for the 128 stations for which CTD data were available. The cluster of stations with thick black lines all had temperatures of $<1.0\,^{\circ}$C at 100 m. The heavy line with a surface temperature of $2.7\,^{\circ}$C represents station KM178. The two dark lines with surface temperatures $>4.0\,^{\circ}$C represent stations KM133 (just south of the Polar Front at approximately 47° W, 55° S) and KM164 (in Drake Passage at approximately 68° W, 60° S). The dashed line is from station YU017, which is located SSE of South Georgia at 38.4° W, 56.8° S.

The marked differences in water column characteristics usually associated with frontal zones are evident in the T/S diagrams and temperature profiles for stations immediately to the north and immediately to the south of the Southern Boundary of the Antarctic Circumpolar Current (SBACC; Fig. 12). This figure illustrates conditions within a transect to the east of South Georgia (Figs. 12A and C) and a transect to the west of South Georgia (Figs. 12B and D). Data from the transect to the east of South Georgia show the

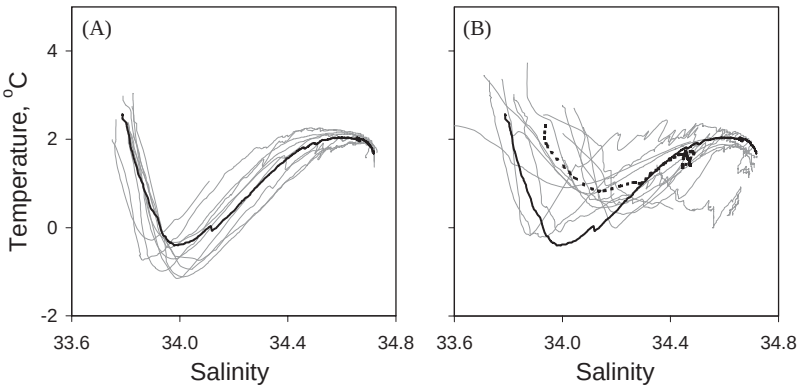

Fig. 11. Apparent mixing of different water masses in the Scotia Sea as evidenced by T/S diagrams. (A) T/S diagrams of ten stations in Drake Passage (light lines) and the mean (dark line), which do not show evidence of any significant mixing with coastal waters. (B) T/S diagrams of 14 stations in the Scotia Sea which indicate significant mixing with other water masses and the mean (dashed line). Surface Chl-*a* concentration at all these stations exceeded 2.5 mg m^{-3}. The mean dark line from (A) is also shown in (B) for comparison.

upper water column to be warmer at the three stations to the north of the SBACC and with evidence of mixing in the upper 300 m, compared to the three stations to the south of the SBACC. The extent of mixing within the SBACC frontal zone appears more pronounced in the transect to the west of South Georgia, as both the temperature profiles and T/S diagrams for the stations to the north of the SBACC indicate interleaving of different water masses. The mean surface Chl-*a* concentration for the five stations to the north of the SBACC was 1.86 mg m^{-3}, compared to 0.71 mg m^{-3} for the stations to the south.

4. Discussion

From the satellite imagery of surface Chl-*a* concentration in the Southern Ocean (Fig. 1), it is evident that phytoplankton biomass is much richer in the Scotia Sea and the Polar Frontal Zone between 10 and 60° W than in other pelagic Antarctic waters. It is likely that this biological richness is related to physical mixing processes involving the different water masses that flow into the Scotia Sea as well as to upwelling of nutrient-rich deep water. These processes are discussed in the following sections in relation to the major environmental factors that might influence the distribution of phytoplankton within the Scotia Sea and over depth within the upper water column.

4.1. Grazing and settling of phytoplankton

Loeb et al. (1997) have shown that losses of phytoplankton biomass due to grazing pressure by krill and salps generally account for <20% of daily primary production and thus would not appear to be a major factor responsible for the spatial variability in Chl-*a* concentration. This view is supported by Kawaguchi et al. (2004) who found no correlation between salp biomass and Chl-*a* in the Scotia Sea during the CCAMLR 2000 Survey, and there appears to be a poor correlation between the phytoplankton data described in this paper and krill abundance in the Scotia Sea as described by Hewitt et al. (2004). Losses of phytoplankton due to sinking out of the euphotic zone also does not appear to be a major factor in the spatial variability of Chl-*a* in the Scotia Sea as data from sediment traps (Karl et al., 1991) and water column Chl-*a* measurements (Holm-Hansen and Mitchell, 1991) have shown that the percentage of primary production lost by sinking is high only during bloom conditions and is generally <26% of total production. However, it is likely that a considerable flux of carbon could sink out of the euphotic zone at the end of a bloom when nutrients become exhausted (Holm-Hansen et al.,

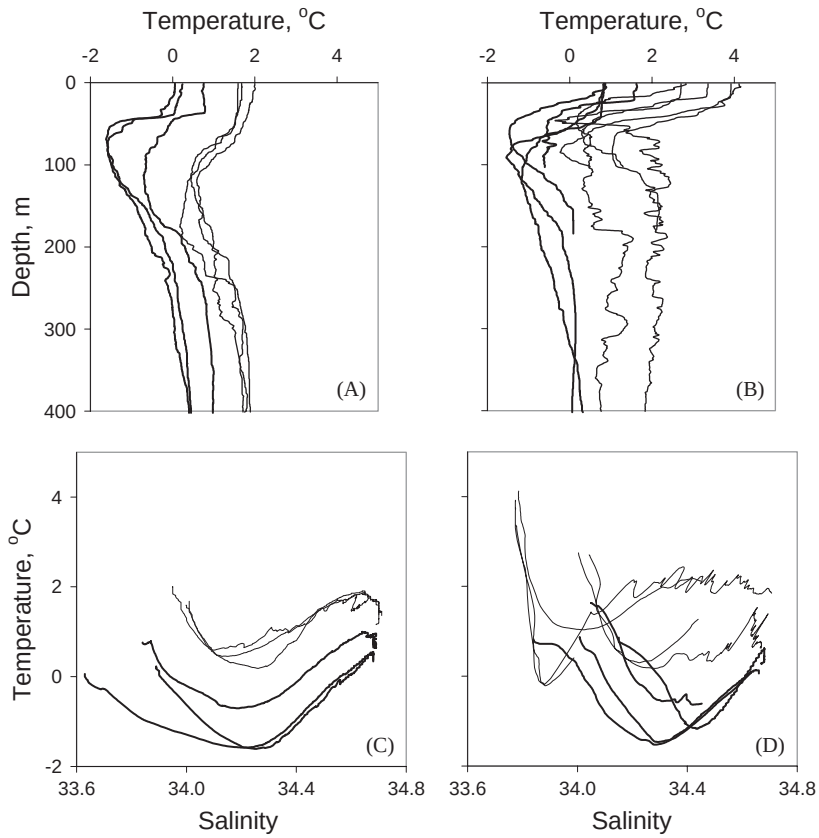

Fig. 12. Temperature profiles (A, B) and T/S diagrams (C, D) for stations located to the north and south of the SBACC as described by Brandon et al. (this volume) for transects SS02 and SS07/08. The SBACC occurred at approximately 32° W, 57° S for SS02 and 43° W, 59° S for SS07/08. (A, C): transect SS02; stations YU08, YU09, and YU10 to the north of the SBACC (light lines), and stations YU11, YU12, and YU13 to the south of the SBACC (dark lines). (B, D): transect SS07/08; stations JCR164, JCR169, JCR184, JCR188, JCR200 to the north of the SBACC (light lines), and stations JCR204, JCR217 and YU28, YU27 to the south of the SBACC (dark lines).

1989). Under non-blooming conditions, much of the daily primary production occurs in nano- and picoplankton (e.g., $<10\,\mu m$) size classes which are little impacted by krill, but rather controlled by microbial grazers (Becquevort, 1997; Burkill et al., 1995; Garrison and Mathot, 1996; Hewes et al., 1985; Rönner et al., 1983). Such 'microbial loop' populations probably contribute little to the sinking flux of organic carbon.

4.2. Light and depth of the upper mixed layer

It is unlikely that light conditions are responsible for the spatial variability in phytoplankton biomass in surface waters within the Scotia Sea for the following reasons. The average daily solar irradiance during January and February around Elephant Island is approximately $650\,\mu Einsteins\,m^{-2}\,s^{-1}$, and the mean irradiance in a 50 m UML is approximately $105\,\mu Einsteins\,m^{-2}\,s^{-1}$ (Helbling et al., 1995). This mean irradiance is close to the saturating light value for photosynthesis (I_k) of $101\,\mu Einsteins\,m^{-2}\,s^{-1}$ as measured by Helbling et al. (1995) and greater than the value of $<100\,\mu Einsteins\,m^{-2}\,s^{-1}$ as reported by Tilzer et al. (1985). The mean depth of the UML during the CCAMLR 2000 Survey was 32 m, so the mean irradiance in the UML would be considerably

greater than the I_k value. As the mean 1% light level in the Scotia Sea is close to 90 m (Helbling et al., 1995) and the compensation light intensity for photosynthesis is close to 0.1% of surface irradiance (Kiefer et al., 1976; Holm-Hansen and Mitchell, 1991), net photosynthesis could still occur throughout the entire depth of the deepest UMLs found during the CCAMLR 2000 Survey.

Previous studies of the relationship between Chl-*a* concentration in surface waters of coastal regions in the Antarctic and UML depth have shown that high Chl-*a* concentrations ($>2.0\,mg\,m^{-3}$) occur only when the UML is shallower than about 40 m (Mitchell and Holm-Hansen, 1991). The lack of correlation between Chl-*a* concentration and UML depth in this study suggests that the factor(s) limiting phytoplankton biomass in Antarctic pelagic waters may be different from the limiting factor(s) in continental shelf waters.

4.3. Temperature effects

Photosynthetic rates increase exponentially with increasing temperature within the temperature range to which cells are adapted (Eppley, 1972). Studies with Antarctic phytoplankton have shown an approximately 30% increase in rates of primary production with an increase in temperature from -1.8 to $4.5\,^{\circ}C$ (Neori and Holm-Hansen, 1982), the range which includes all 137 CCAMLR 2000 Survey stations. However, Chl-*a* concentration (Fig. 3) during this study did not show a positive correlation with the water temperature gradients reported by Brandon et al. (2004). This suggests that other environmental factors in the Scotia Sea are more important than the direct effect of temperature on phytoplankton growth rates.

4.4. Inorganic nutrients and physical mixing processes

Many studies on the concentrations of macronutrients that limit phytoplankton biomass in temperate and tropical waters (nitrogen, phosphorus, silicon) indicate that concentrations in Antarctic waters are in excess of phytoplankton requirements, and would not limit phytoplankton biomass. The only known exceptions are when phytoplankton blooms in coastal waters exceed $25\,mg\,Chl\text{-}a\,m^{-3}$ (e.g., Holm-Hansen et al., 1989; Kocmur et al., 1990) and near the Polar Front, where silicon concentrations may be $<10\,\mu M$ (Atkinson et al., 2001; Jacques, 1983; Whitehouse et al., 2000). It is unlikely that these elements were limiting phytoplankton biomass during the CCAMLR 2000 Survey, as previous studies have reported high concentrations of nitrogen, phosphorus, and silicon in Drake Passage and the Scotia Sea (Biggs et al., 1982; Silva et al., 1995).

The situation is very different, however, in relation to the concentration of iron (Fe), which is an essential micronutrient for phytoplankton. Both direct and indirect evidence indicate that Fe limits phytoplankton biomass in pelagic Antarctic waters. There are insufficient data at present to establish whether Fe also limits phytoplankton biomass in coastal waters, but Sedwick et al. (2000) have shown that low concentrations of Fe may limit phytoplankton growth during mid- to late summer in shelf waters of the Ross Sea. Support for the hypothesis that Fe is important in limiting phytoplankton biomass in at least some Antarctic waters includes the following.

1. Studies on Fe requirements by phytoplankton indicate that the cellular carbon/Fe ratio (by weight) is usually in the range 2000–10,000 (Bruland et al., 2001; de Baar et al., 1990; Löscher et al., 1997; Maldonado et al., 2001; Morel et al., 1991), which would suggest that a concentration of 0.1 nM Fe in pelagic Antarctic waters would support a phytoplankton biomass of approximately 10 to $50\,mg\,C\,m^{-3}$, or 0.2 to $1.0\,mg\,Chl\text{-}a\,m^{-3}$. Iron concentrations in pelagic Antarctic waters, including the Bellingshausen Sea, Drake Passage, Ross Sea, and the Scotia Sea, are generally in the range <0.05–$0.20\,nM$ (de Baar et al., 1999; Fitzwater et al., 2000; Martin et al., 1990a; Timmermans et al., 1998). In contrast, Antarctic waters overlying continental shelves may have relatively high Fe concentrations, in the range 1–10 nM, which would support phytoplankton blooms (Fitzwater et al., 2000; Martin et al., 1990a, 1991; Nolting et al., 1991; Westerland

and Öhman, 1991). Fitzwater et al. (2000) have shown that elevated concentrations of Fe in surface waters of the Ross Sea coincide with increased biomass of phytoplankton.

2. Incubation experiments with Antarctic pelagic water samples have shown that addition of excess Fe (usually 1–10 nM) results in significantly higher Chl-*a* concentrations within six to ten days relative to control samples (Buma et al., 1991; Helbling et al., 1991; Martin et al., 1990b). Similar experiments using water samples from coastal regions do not show such an increase in phytoplankton biomass relative to control samples (Buma et al., 1991; de Baar et al., 1990; Helbling et al., 1991; Martin et al., 1991). Franck et al. (2003) have also shown that addition of Fe to natural phytoplankton assemblages in pelagic waters of the Southern Ocean significantly increased the uptake rates of silicic acid and nitrate.
3. Addition of large quantities of Fe to a localized area of pelagic Antarctic waters results in the development of phytoplankton blooms that are confined to the area of Fe enrichment (Boyd et al., 2000; Maldonado et al., 2001; Smetacek, 2001). Waters surrounding Fe-enriched patches do not show similar increases in Chl-*a* concentration.
4. Indirect evidence of nutrient limitation in pelagic Antarctic waters with very low concentrations of Chl-*a* in surface areas (e.g., the purple areas in Fig. 1) is provided by the distribution of Chl-*a* in the upper 100 m of the water column (Holm-Hansen et al., 1994). As seen in Fig. 5A, there is a deep Chl-*a* maximum at approximately 75 m. Such a profile is similar to the distribution of Chl-*a* in the oligotrophic north Pacific gyre, where nitrogen and phosphorus are below conventional detection limits in the upper water column, and the Chl-*a* maximum occurs within the nutricline at approximately 120 m (Kiefer et al., 1976). As nitrogen and phosphorus are in excess concentrations in Antarctic waters, it seems likely that the Chl-*a* maximum seen in Fig. 5A resides within the ferrocline. An increase in Fe with depth has been documented by many studies (e.g., de Baar et al., 1999; Fitzwater et al., 2000; Martin et al., 1990a; Westerland and Öhman, 1991).

These studies on Fe in the Southern Ocean all suggest that ACC waters usually have low Fe concentrations and low Chl-*a* concentrations, unless enriched by Fe from other sources. The major Fe input to surface waters of the ACC is by upward transport from deeper waters, with only minor contributions from atmospheric aerosols (Löscher et al., 1997). High Chl-*a* areas are generally restricted to coastal regions (with high Fe concentrations) or to localized deep water areas which have probably been enriched by Fe from upwelling or from eddies originating from continental shelf regions. The distribution of Chl-*a* in the upper water column at all stations during the CCAMLR 2000 Survey shows the following relationships with temperature and salinity and supports the view that the richness of the Scotia Sea is related to the input of Fe into the euphotic zone by mixing with Fe-rich coastal waters or from upwelling of deeper waters.

1. The regions with the lowest Chl-*a* concentration are Drake Passage and the area between 20 and 25° W and 57 and 63° S (the purple areas in Fig. 1). Stations in Drake Passage show relatively little mixing; the T/S diagrams are reasonably uniform and similar in space (Fig. 11A) to those reported by Brandon et al. (2004) in the detailed profile across Drake Passage. These T/S diagrams are similar to those for Drake Passage stations with high nitrogen/silicon ratios (Holm-Hansen et al., 1997) and where Fe was limiting phytoplankton biomass (Helbling et al., 1991). The remnants of the Winter Water in the temperature profiles for stations between 20 and 25° W and 57 and 63° S is shown by temperatures of $<1.0\,^{\circ}C$ (Fig. 10) and there is little or no evidence of erosion of this cold water layer. Most of the stations in these areas showed low Chl-*a* concentration throughout the euphotic zone (Figs. 5A and B).
2. Fig. 1 shows high Chl-*a* values in the area between 55 and 60° W and 58 and 60° S (NNW of Elephant Island), and extremely low Chl-*a* values immediately to the west of this area.

Water flow in this region is strongly influenced by the Shackleton Fracture Zone (SFZ, see Fig. 2A) which rises to depths mostly between 1000 and 2000 m, but with some areas of <1000 m (Sievers and Nowlin, 1988; Stein, 1988). There is a deep channel of >3000 m between the southern end of the SFZ and Elephant Island. The SFZ appears to cause a change in the main flow of the ACC to the north and northeast, although with some deep flow passing to the south of the SFZ (see purple areas, Fig. 1). Physical oceanographic measurements and buoy drift tracks in this area have shown that Bransfield Strait and Weddell Sea waters flow in a northwesterly direction to the east and north of Elephant Island (Hofmann et al. 1996, 1998; Ichii and Naganobu, 1996; Stein, 1988). This mixing of Drake Passage waters with Fe-enriched coastal waters near the SFZ may result in the phytoplankton-enriched waters evident to the north and northeast of Elephant Island (Fig. 3; see also Holm-Hansen et al., 2004).

3. Most of the stations in the central Scotia Sea show evidence of mixing (see Figs. 10 and 11B). Nearly all these stations had high Chl-*a* concentrations (see Fig. 1). Waters flowing into and mixing within the Scotia Sea include major contributions from the ACC, Bransfield Strait, and the Weddell Sea (see Fig. 2B). The major outflow of Weddell Sea water is to the northwest of the South Orkney Islands where it merges with ACC waters. Although the front between Drake Passage and Weddell Sea waters is clearly defined in that area, it is not clearly defined elsewhere in the Scotia Sea, and instead appears in the form of eddy-like structures which increase in size downstream with the flow in a northeasterly direction (Foster and Middleton, 1984). Orsi et al. (1993) have described other locations to the east of the South Orkney Islands where Weddell Sea waters flow northward to mix with ACC waters. In addition to Fe enrichment by mixing with coastal waters, the euphotic zone in pelagic waters also might be enriched by upwelling associated with submarine mountain ranges, isolated sea mounts, and plateaus, even though these bathymetric features may be >2000 m in depth (Atkinson et al., 2001; Hayes et al., 1984; Moore et al., 1999; Orsi et al., 1995; Sievers and Nowlin, 1988; Stein, 1988). Hayes et al. (1984) and Sullivan et al. (1993) report that phytoplankton biomass is often enhanced near underwater plateaus and ridges. It should be noted that there are many such features in the Scotia Sea to the north of the South Orkney Islands and to the southwest of South Georgia.
4. High Chl-*a* values are often associated with frontal mixing zones, presumably owing to upwelling (e.g., de Baar et al., 1995; Löscher et al., 1997). Figs. 12B and D illustrate the marked differences in Chl-*a* values and temperature and salinity characteristics in the upper water column across the SBACC. The temperature profiles to the north of the SBACC indicate considerable mixing relative to stations to the south of the SBACC and such mixing was also evident in the T/S diagrams. The stations where much mixing had occurred had a mean Chl-*a* value in surface waters of $1.86\,\mathrm{mg\,m^{-3}}$, compared to $0.71\,\mathrm{mg\,m^{-3}}$ at stations to the south.

5. Conclusions

A survey of Chl-*a* distribution in the Scotia Sea and Drake Passage during the austral summer of 2000, by four research vessels and using satellite imagery, showed much horizontal and vertical variability in phytoplankton biomass. An excellent relationship ($r^2 = 0.92$) was found between surface and integrated Chl-*a* concentration, indicating that satellite imagery of surface Chl-*a* concentration also provides a good interpretation of integrated Chl-*a* values. Estimates by two different methods of rates of primary production based on Chl-*a* concentration were 597 and $994\,\mathrm{mg\,C\,m^{-2}\,day^{-1}}$ for the entire Scotia Sea during January and February. These values are much higher than most productivity measurements for pelagic Antarctic waters, which are generally in the range $100–200\,\mathrm{mg\,C\,m^{-2}\,day^{-1}}$ (El-Sayed, 1988; Holm-Hansen et al., 1977). High Chl-*a* concentrations were found near shelves associated

with land masses and in the central Scotia Sea. Although Fe concentrations were not measured during the CCAMLR 2000 Survey, it is likely that Fe availability controls phytoplankton biomass in the pelagic Scotia Sea since high Chl-*a* concentrations were associated with temperature and density profiles that indicated mixing between ACC waters and Fe-enriched waters originating from coastal regions or from upwelling of deeper waters associated with bathymetric features such as the SFZ. Other factors thought to control phytoplankton biomass, namely grazing, settling, light, and temperature, do not appear to account for the great spatial variability in Chl-*a* distribution observed during this study.

References

Amos, A.F., 2001. A decade of oceanographic variability in summertime near Elephant Island, Antarctica. Journal of Geophysical Research 106 (C10), 22,401–22,423.

Atkinson, A., Whitehouse, M.J., Priddle, J., Cripps, G.C., Ward, P., Brandon, M.A., 2001. South Georgia, Antarctica: a productive, cold water, pelagic ecosystem. Marine Ecology Progress Series 216, 279–308.

Becquevort, S., 1997. Nanoprotozooplankton in the Atlantic sector of the Southern Ocean during early spring: biomass and feeding activities. Deep-Sea Research II 44, 355–373.

Behrenfeld, M.J., Falkowski, P.G., 1997. Photosynthetic rates derived from satellite-based chlorophyll concentration. Limnology and Oceanography 42, 1–20.

Biggs, D.C., Johnson, M.A., Bidigare, R.R., Guffy, J.D., Holm-Hansen, O., 1982. Shipboard autoanalyzer studies of nutrient chemistry, 0–200 m, in the eastern Scotia Sea during FIBEX (January–March, 1981). Texas A&M University, Department Oceanography Technical Reports, 88-11-T.

Boyd, P.W., plus 34 co-authors, 2000. A mesoscale phytoplankton bloom in the polar Southern Ocean stimulated by Fe fertilization. Nature 407, 695–702.

Brandon, M.A., Naganobu, M., Demer, D.A., Chernyshkov, P., Trathan, P.N., Thorpe, S.E., Kameda, T., Berezhinskiy, O.A., Hawker, E.J., Grant, S., 2004. Physical oceanography in the Scotia Sea during the CCAMLR 2000 survey, austral summer 2000. Deep-Sea Research II, this issue [doi: 10.1016/j.dsr2.2004.06.006].

Bruland, K.W., Rue, E.L., Smith, G.J., 2001. Iron and macronutrients in California coastal upwelling regimes: implications for diatom blooms. Limnology and Oceanography 46, 1661–1674.

Buma, A.G.J., de Baar, H.J.W., Nolting, R.F., van Bennekom, A.J., 1991. Metal enrichment experiments in the Weddell–Scotia seas: effects of iron and manganese on various plankton communities. Limnology and Oceanography 36, 1865–1878.

Burkill, P.H., Edwards, E.S., Sleigh, M.A., 1995. Microzooplankton and their role in controlling phytoplankton growth in the marginal ice zone of the Bellingshausen Sea. Deep-Sea Research II 42, 1277–1290.

de Baar, H.J.W., Buma, A.G.J., Nolting, R.F., Cadee, G.C., Jacques, G., Treguer, P.J., 1990. On iron limitation of the Southern Ocean: experimental observations in the Weddell and Scotia Seas. Marine Ecology Progress Series 65, 105–122.

de Baar, H.J.W., de Jong, J.T.M., Bakker, D.C.E., Löscher, B.M., Veth, C., Bathmann, U., Smetacek, V., 1995. Importance of iron for plankton blooms and carbon dioxide drawdown in the Southern Ocean. Nature 373, 412–415.

de Baar, H.J.W., de Jong, J.T.M., Nolting, R.F., Timmermans, K.R., van Leeuwe, M.A., Bathman, U., van der Loeff, M.R., Sildam, J., 1999. Low dissolved Fe and the absence of diatom blooms in remote Pacific waters of the Southern Ocean. Marine Chemistry 66, 1–34.

El-Sayed, S.Z., 1988. Productivity of the Southern Ocean: a closer look. Comparative Biochemistry and Physiology 90B, 489–498.

El-Sayed, S.Z., Weber, L.H., 1982. Spatial and temporal variations in phytoplankton biomass and primary productivity in the southwest Atlantic and the Scotia Sea. Polar Biology 1, 83–90.

Eppley, R.W., 1972. Temperature and phytoplankton growth in the sea. Fishery Bulletin 70, 1063–1085.

Fisheries Agency, 1989. Report of the Fifth Antarctic Ocean Survey Cruise of JFA R/V Kaiyo Maru in 1987/88 (in Japanese). The Fisheries Agency of Japan, 301pp.

Fitzwater, S.E., Johnson, K.S., Gordon, R.M., Coale, K.H., Smith, W.O., 2000. Trace metal concentrations in the Ross Sea and their relationship with nutrients and phytoplankton growth. Deep-Sea Research II 47, 3159–3179.

Foster, T.D., Middleton, J.H., 1984. The oceanographic structure of the eastern Scotia Sea—I. Physical oceanography. Deep-Sea Research 31, 529–550.

Franck, V.M., Bruland, K.W., Hutchins, D.A., Brzezinski, M.A., 2003. Iron and zinc effects on silicic acid and nitrate uptake kinetics in three high-nutrient, low chlorophyll (HPLC) regions. Marine Ecology Progress Series 252, 15–33.

Garrison, D.L., Mathot, S., 1996. Pelagic and sea ice microbial communities. In: Ross, R.M., Hofmann, E.E., Quetin, L.B. (Eds.), Foundations for Ecological Research West of the Antarctic Peninsula. Antarctic Research Series,, vol. 70. American Geophysical Union, Washington, DC, pp. 155–172.

Gordon, A.L., Baker, T.N., 1982. Southern Ocean Atlas. Columbia University Press, New York.

Hayes, P.K., Whitaker, T.M., Fogg, G.E., 1984. The distribution and nutrient status of phytoplankton in the Southern Ocean between 20 and 70° W. Polar Biology 3, 153–165.

Helbling, E.W., Villafane, V., Holm-Hansen, O., 1991. Effect of Fe on productivity and size distribution of Antarctic

phytoplankton. Limnology and Oceanography 36, 1879–1885.

Helbling, E.W., Villafañe, V.E., Holm-Hansen, O., 1995. Variability of phytoplankton distribution and primary production around Elephant Island, Antarctica, during 1990–1993. Polar Biology 15, 233–246.

Hewes, C.D., Holm-Hansen, O., Sakshaug, E., 1985. Alternate carbon pathways at lower trophic levels in the Antarctic food web. In: Siegfried, W.R., Condy, P.R., Laws, R.M. (Eds.), Antarctic Nutrient Cycles and Food Webs. Springer, Heidelberg, pp. 277–283.

Hewitt, R.P., Kim, S., Naganobu, M., Gutierrez, M., Kang, D., Takao, Y., Quinones, J., Lee, Y.-H., Shin, H.-C., Kawaguchi, S., Emery, J.H., Demer, D.A., Loeb, V.J., 2004. Variation in the biomass density and demography of Antarctic krill in the vicinity of the South Shetland Islands during the 1999/2000 austral summer. Deep-Sea Research II, this issue [doi: 10.1016/j.dsr2.2004.06.018].

Hofmann, E.E., Klinck, J.M., Lascara, C.M., Smith, D.A., 1996. Water mass distribution and circulation west of the Antarctic Peninsula and including Bransfield Strait. In: Ross, R.M., Hofmann, E.E., Quetin, L.B. (Eds.), Foundations for Ecological Research West of the Antarctic Peninsula. Antarctic Research Series,, vol. 70. American Geophysical Union, Washington, DC, pp. 61–80.

Hofmann, E.E., Klinck, J.M., Locarnini, R.A., Fach, B., Murphy, E., 1998. Krill transport in the Scotia Sea and environs. Antarctic Science 10, 406–415.

Holm-Hansen, O., Mitchell, B.G., 1991. Spatial and temporal distribution of phytoplankton and primary production in the western Bransfield Strait region. Deep-Sea Research 38, 961–980.

Holm-Hansen, O., Lorenzen, C.J., Holmes, R.W., Strickland, J.D.H., 1965. Fluorometric determination of chlorophyll. Journal du Conseil International pour l' Exploration de la Mer 30, 3–15.

Holm-Hansen, O., El-Sayed, S.Z., Franceschini, G.A., Cuhel, R.L., 1977. Primary production and the factors controlling phytoplankton growth in the Southern Ocean. In: Llano, G.A. (Ed.), Adaptations Within Antarctic Ecosystems. Proceedings of the Third SCAR Symposium on Antarctic Biology. Gulf Publishing Co., Houston, TX, pp. 11–50.

Holm-Hansen, O., Mitchell, B.G., Hewes, C.D., Karl, D.M., 1989. Phytoplankton blooms in the vicinity of Palmer Station, Antarctica. Polar Biology 10, 49–57.

Holm-Hansen, O., Amos, A.F., Silva, N., Villafañe, V., Helbling, E.W., 1994. In situ evidence for a nutrient limitation of phytoplankton growth in pelagic Antarctic waters. Antarctic Science 6, 315–324.

Holm-Hansen, O., Hewes, C.D., Villafañe, V.E., Helbling, E.W., Silva, N., Amos, T., 1997. Distribution of phytoplankton and nutrients in relation to different water masses in the area around Elephant Island, Antarctica. Polar Biology 18, 145–153.

Holm-Hansen, O., Kahru, M., Hewes, C.D., Kawaguchi, S., Kameda, T., Sushin, V.A., Krasovski, I., Priddle, J., Korb, R., Hewitt, R.P., Mitchell, B.G., 2004. Temporal and spatial distribution of chlorophyll-*a* in surface waters of the Scotia Sea as determined by both shipboard measurements and satellite data. Deep-Sea Research II, this issue [doi: 10.1016/j.dsr2.2004.06.004].

Ichii, T., Naganobu, M., 1996. Surface water circulation in krill fishing areas near the south Shetland Islands. CCAMLR Science 3, 125–136.

Jacques, G., 1983. Some ecophysiological aspects of the Antarctic phytoplankton. Polar Biology 2, 27–33.

Karl, D.M., Tilbrook, B.D., Tien, G., 1991. Seasonal coupling of organic matter production and particle flux in the western Bransfield Strait, Antarctica. Deep-Sea Research 38, 1097–1126.

Kawaguchi, S., Siegel, V., Litvinov, F.F., Loeb, V.J., Watkins, J.L., 2004. Salp distribution and size composition in the Atlantic sector of the Southern Ocean. Deep-Sea Research II, this issue [doi: 10.1016/j.dsr2.2004.06.017].

Kiefer, D.A., Olson, R.J., Holm-Hansen, O., 1976. Another look at the nitrite and chlorophyll maxima in the central North Pacific. Deep-Sea Research 23, 1199–1208.

Kocmur, S.F., Vernet, M., Holm-Hansen, O., 1990. RACER: nutrient depletion by phytoplankton during the 1989 austral spring bloom. Antarctic Journal of the United States 25, 138–141.

Loeb, V., Siegel, V., Holm-Hansen, O., Hewitt, R., Fraser, W., Trivelpiece, W., Trivelpiece, S., 1997. Effects of sea-ice extent and krill or salp dominance on the Antarctic food web. Nature 387, 897–900.

Löscher, B.M., de Baar, H.J.W., de Jong, J.T.M., Veth, C., Dehairs, F., 1997. The distribution of Fe in the Antarctic Circumpolar Current. Deep-Sea Research II 44, 143–187.

Maldonado, M.T., Boyd, P.W., LaRoche, J., Strzepek, R., Waite, A., Bowie, A.R., Croot, P.L., Frew, R.D., Price, N.M., 2001. Iron uptake and physiological response of phytoplankton during a mesoscale Southern Ocean iron enrichment. Limnology and Oceanography 46, 1802–1808.

Martin, J.H., Gordon, R.M., Fitzwater, S.E., 1990a. Iron in Antarctic waters. Nature 345, 156–158.

Martin, J.H., Fitzwater, S.E., Gordon, R.M., 1990b. Iron deficiency limits phytoplankton growth in Antarctic waters. Global Biogeochemical Cycles 4, 5–12.

Martin, J.H., Gordon, R.M., Fitzwater, S.E., 1991. The case for iron. Limnology and Oceanography 36, 1793–1802.

McClain, C.R., Cleave, M.L., Feldman, G.C., Gregg, W.W., Hooker, S.B., Kuring, N., 1998. Science quality SeaWiFS data for global biosphere research. Sea Technology 39(9), 10–16.

Mitchell, B.G., Holm-Hansen, O., 1991. Observations and modeling of the Antarctic phytoplankton crop in relation to mixing depth. Deep-Sea Research 38, 981–1007.

Mitchell, B.G., Brody, E.A., Holm-Hansen, O., McClain, C., Bishop, J., 1991. Light limit of phytoplankton crop size and residual macro-nutrients in the Southern Ocean. Limnology and Oceanography 36, 1662–1677.

Moore, J.K., Abbott, M.R., Richman, J.G., Smith, W.O., Cowles, T.J., Coale, K.H., Gardner, W.D., Barber, R.T.,

1999. SeaWIFS satellite ocean color data from the Southern Ocean. Geophysical Research Letters 26, 1465–1468.

Morel, A., Berthon, J.-F., 1989. Surface pigments, algal biomass profiles, and potential production of the euphotic layer: relationships reinvestigated in view of remote-sensing applications. Limnology and Oceanography 34, 1545–1562.

Morel, F.M.M., Rueter, J.G., Price, N.M., 1991. Iron nutrition of phytoplankton and its possible importance in the ecology of ocean regions with high nutrient and low biomass. Oceanography 4, 56–61.

Neori, A., Holm-Hansen, O., 1982. Effect of temperature on rate of photosynthesis in Antarctic phytoplankton. Polar Biology 1, 33–38.

Nolting, R.F., de Baar, H.J.W., van Bennekom, A.J., Masson, A., 1991. Cadmium, copper and iron in the Scotia Sea, Weddell Sea/Scotia Confluence (Antarctica). Marine Chemistry 35, 219–243.

O'Reilly, J.E., Maritorena, S., Mitchell, B.G., Siegel, D.A., Carder, K.L., Garver, S.A., Kahru, M., McClain, C., 1998. Ocean color chlorophyll algorithms for SeaWiFS. Journal of Geophysical Research 103, 24,937–24,953.

O'Reilly, J.E., et al., 2000. Ocean color chlorophyll a algorithms for SeaWiFS, OC2, and OC4: Version 4. In: Hooker, S.B., Firestone, E.R. (Eds.), SeaWiFS Postlaunch Calibration and Validation Analyses, Part 3. National Aeronautics and Space Administration Technical Memorandum 2000-206892, vol. 11, pp. 9–23.

Orsi, A.H., Nowlin Jr., W.D., Whitworth III, T., 1993. On the circulation and stratification of the Weddell Gyre. Deep-Sea Research I 40, 169–203.

Orsi, A.H., Whitworth III, T., Nowlin Jr., W.D., 1995. On the meridional extent and fronts of the Antarctic Circumpolar Current. Deep-Sea Research I 42, 641–673.

Rönner, U., Sörensson, F., Holm-Hansen, O., 1983. Nitrogen assimilation by phytoplankton in the Scotia Sea. Polar Biology 2, 137–147.

Sakshaug, E., Slagstad, D., Holm-Hansen, O., 1991. Factors controlling the development of phytoplankton blooms in the Antarctic Ocean—a mathematical model. Marine Chemistry 35, 259–271.

Sedwick, P.N., DiTullio, G.R., Mackey, D.J., 2000. Iron and manganese in the Ross Sea, Antarctica: seasonal iron limitation in Antarctic shelf waters. Journal of Geophysical Research 105 (C5), 11,321–11,336.

Sievers, H.A., Nowlin Jr., W.D., 1988. Upper ocean characteristics in Drake Passage and adjoining areas of the Southern Ocean, 39° W-95° W. In: Sahrhage, D. (Ed.), Antarctic Ocean and Resources Variability. Springer, Berlin, pp. 57–80.

Silva, S.N., Helbling, E.W., Villafañe, V., Amos, A.F., Holm-Hansen, O., 1995. Variability in nutrient concentrations around Elephant Island, Antarctica, during 1991–1993. Polar Research 14, 69–82.

Smetacek, V., 2001. EisenEx: International Team Conducts Iron Experiment in Southern Ocean. United States JGOFS newsletter, January, 11–14.

Stein, M., 1988. Variation of geostrophic circulation off the Antarctic Peninsula and in the southwest Scotia Sea, 1975–1985. In: Sahrhage, D. (Ed.), Antarctic Ocean and Resources Variability. Springer, Berlin, pp. 81–91.

Sullivan, C.W., Arrigo, K.R., McClain, C.R., Comiso, J.C., Firestone, J., 1993. Distributions of phytoplankton blooms in the Southern Ocean. Science 262, 1832–1837.

Tilzer, M.M., von Bodungen, B., Smetacek, V., 1985. Light-dependence of phytoplankton photosynthesis in the Antarctic Ocean: implications for regulating productivity. In: Siegfried, W.R., Condy, P.R., Laws, R.M. (Eds.), Antarctic Nutrient Cycles and Food Webs. Springer, Heidelberg, pp. 60–69.

Timmermans, K.R., van Leeuwe, M.A., de Jong, J.T.M., McKay, R.M.L., Nolting, R.F., Witte, H.J., van Ooyen, J., Swagerman, M.J.W., Kloosterhuis, H., de Baar, H.J.W., 1998. Iron stress in the Pacific region of the Southern Ocean: evidence from enrichment bioassays. Marine Ecology Progress Series 166, 27–41.

Watkins, J.L., Hewitt, R.P., Naganobu, M., Sushin, V.A., 2004. The CCAMLR 2000 Survey: a multinational, multi-ship biological oceanography survey of the Atlantic sector of the Southern Ocean. Deep-Sea Research II, this issue [doi: 10.1016/j.dsr2.2004.06.010].

Westerland, S., Öhman, P., 1991. Iron in the water column of the Weddell Sea. Marine Chemistry 35, 199–217.

Whitehouse, M.J., Priddle, J., Brandon, M.A., 2000. Chlorophyll/nutrient characteristics in the water masses to the north of South Georgia, Southern Ocean. Polar Biology 23, 373–382.